© 2015. Published by The Company of Biologists Ltd | Development (2015) 142, 1267-1278 doi:10.1242/dev.111526

RESEARCH ARTICLE

STEM CELLS AND REGENERATION

Duration of culture and sonic hedgehog signaling differentially specify PV versus SST cortical interneuron fates from embryonic stem cells

Jennifer A. Tyson[1,2], Ethan M. Goldberg[3,4], Asif M. Maroof[5], Qing Xu[6], Timothy J. Petros[7] and Stewart A. Anderson[1,*]

ABSTRACT

Medial ganglionic eminence (MGE)-derived GABAergic cortical interneurons (cINs) consist of multiple subtypes that are involved in many cortical functions. They also have a remarkable capacity to migrate, survive and integrate into cortical circuitry after transplantation into postnatal cortex. These features have engendered considerable interest in generating distinct subgroups of interneurons from pluripotent stem cells (PSCs) for the study of interneuron fate and function, and for the development of cell-based therapies. Although advances have been made, the capacity to generate highly enriched pools of subgroup fate-committed interneuron progenitors from PSCs has remained elusive. Previous studies have suggested that the two main MGE-derived interneuron subgroups – those expressing somatostatin (SST) and those expressing parvalbumin (PV) – are specified in the MGE from Nkx2.1-expressing progenitors at higher or lower levels of sonic hedgehog (Shh) signaling, respectively. To further explore the role of Shh and other factors in cIN fate determination, we generated a reporter line such that Nkx2.1-expressing progenitors express mCherry and postmitotic Lhx6-expressing MGE-derived interneurons express GFP. Manipulations of Shh exposure and time in culture influenced the subgroup fates of ESC-derived interneurons. Exposure to higher Shh levels, and collecting GFP-expressing precursors at 12 days in culture, resulted in the strongest enrichment for SST interneurons over those expressing PV, whereas the strongest enrichment for PV interneurons was produced by lower Shh and by collecting mCherry-expressing cells after 17 days in culture. These findings confirm that fate determination of cIN subgroups is crucially influenced by Shh signaling, and provide a system for the further study of interneuron fate and function.

KEY WORDS: Cortical interneurons, Embryonic stem cells, Fate specification, Parvalbumin, Somatostatin, Sonic hedgehog, Mouse

INTRODUCTION

In the mammalian neocortex, GABAergic cortical interneurons (cINs) facilitate cognition by providing inhibitory inputs to cortical circuitry (Lehmann et al., 2012; Fino et al., 2013). Consequently, interneuron dysfunction is associated with a variety of neurological diseases, including seizure disorders, schizophrenia and autism (Belforte et al., 2010; Chao et al., 2010; Inan et al., 2013). Interneurons are classified into functionally distinct subgroups based on neurochemical markers, connectivity profiles and electrophysiological properties (DeFelipe et al., 2013), with specific subtypes being implicated in different disease etiologies (Binaschi et al., 2003; Levitt et al., 2004; Inan et al., 2013; Jiang et al., 2013; Smith-Hicks, 2013). Genetic fate mapping and transplantation studies have revealed that cINs arise from the ganglionic eminences (GEs) of the subcortical telencephalon. Nearly all of these can be divided into non-overlapping subgroups that express one of three markers: parvalbumin (PV; Pvalb – Mouse Genome Informatics) or somatostatin (SST), which originate in the medial ganglionic eminence (MGE), and 5HT3aR, which originates in the caudal ganglionic eminence (Lee et al., 2010; Rudy et al., 2011). Together, the PV and SST-expressing subgroups, which have distinct electrophysiological and axon-targeting properties (Kawaguchi and Kubota, 1997; Batista-Brito and Fishell, 2009), constitute ~60% of all cINs in the mouse frontal cortex (Tamamaki et al., 2003; Xu et al., 2010b). These MGE-derived interneurons require the expression of the transcription factor Nkx2.1 during the progenitor stage (Sussel et al., 1999; Xu et al., 2004; Butt et al., 2008), then downregulate this gene to facilitate migration into the cortex (Nóbrega-Pereira et al., 2008). Upstream of Nkx2.1, sonic hedgehog (Shh) is required for the induction and maintenance of Nkx2.1 (Xu et al., 2005), and higher levels of Shh bias MGE progenitors to SST-expressing interneuron fates, whereas lower levels bias for the PV-expressing subgroup [(Xu et al., 2010a); but see also (Flandin et al., 2011)]. Downstream of Nkx2.1, its direct target Lhx6 is maintained in MGE-derived interneurons from cell cycle exit through postnatal development and is necessary for their normal development (Lavdas et al., 1999; Sussel et al., 1999; Liodis et al., 2007; Du et al., 2008; Zhao et al., 2008; Flandin et al., 2011; Vogt et al., 2014).

Due to their remarkable ability to migrate, integrate and influence local activity after transplantation into the postnatal brain, there has been considerable interest in deriving cINs from pluripotent stem cells (PSCs) to be used in cell-based therapies for interneuron-related diseases (Goulburn et al., 2012; Southwell et al., 2014; Tyson and Anderson, 2014). Protocols have been established to derive these neurons from both mouse and human PSCs (Watanabe et al., 2005; Goulburn et al., 2011; Maroof et al., 2010, 2013; Danjo et al., 2011; Au et al., 2013; Chen et al., 2013; Nicholas et al., 2013; Petros et al., 2013). However, despite the relevance to cell-based therapies, progress in generating enriched populations of interneuron subgroups has been slow. Recently, success in increasing the generation of PV relative to SST-expressing interneurons was achieved by expression of Lmo3 after expression of Nkx2.1 and Dlx2 (Au et al., 2013). Here, we test the hypothesis that, if PSC differentiation parallels key aspects

[1]Department of Psychiatry, Children's Hospital of Philadelphia, University of Pennsylvania School of Medicine ARC 517, Philadelphia, PA 19104-5127, USA. [2]Department of Psychiatry, Weill Medical College of Cornell University, New York, NY 10021, USA. [3]Division of Neurology, The Children's Hospital of Philadelphia, University of Pennsylvania, Philadelphia, PA 19083, USA. [4]Department of Neurology, Perelman School of Medicine, University of Pennsylvania, Philadelphia, PA 19083, USA. [5]Harvard University Department of Stem Cell and Regenerative Biology, Cambridge, MA 02138, USA. [6]Center for Genomics and Systems Biology, New York University Abu Dhabi, Abu Dhabi, United Arab Emirates. [7]Department of Neuroscience, NYU Langone Medical Center, New York, NY 10016, USA.

*Author for correspondence (sande@mail.med.upenn.edu)

Received 20 May 2014; Accepted 2 February 2015

Development (2015) 142, 1267-1278 doi:10.1242/dev.111526

of native interneuron development, manipulation of Shh signaling, together with the timing of collection of interneuron precursors, should enrich for SST or PV interneuron subgroups without the need for transgenic expression of fate-determining factors. Indeed, a higher level of Shh exposure and earlier harvest of interneuron precursors allows for a roughly 4:1 bias for SST-expressing interneurons, whereas low Shh signaling conditions and later harvest results in a similar bias for the PV subgroup. These findings confirm that fate determination of cIN subgroups is crucially influenced by Shh signaling. In addition, we provide a system for the further study of interneuron fate and function, as well as for the development of interneuron subgroup-selective transplantation therapies for treating a variety of neurological disorders, in which dysfunctional GABAergic signaling is a shared pathological mechanism.

RESULTS

Efficient telencephalic patterning in mESCs

Previous studies have generated cIN-like cells from mESCs (Watanabe et al., 2005; Maroof et al., 2010; Danjo et al., 2011; Maisano et al., 2012; Au et al., 2013; Chen et al., 2013; Petros et al., 2013). However, a protocol to efficiently enrich for pallidal telencephalic progenitors, as evidenced by a majority of cells expressing transcription factors Foxg1 and Nkx2.1, has been elusive. Consequently, we sought to improve the telencephalic induction in our differentiation paradigm. An organized cross-regulation of Shh and Wnt signaling is required for normal forebrain development, whereby Wnts are strongly expressed in the dorsal and caudal domains of the developing central nervous system (CNS) (Gaspard and Vanderhaeghen, 2011; Houart et al., 2002; Ohkubo et al., 2002; Shimogori et al., 2004; Hébert and Fishell, 2008) (schematized in Fig. 1A,Aa). In the mouse embryo, Dkk1 is an endogenous Wnt inhibitor (Glinka et al., 1998), in which a signaling gradient of Wnt/β-catenin and Dkk1 mediates anterior-posterior (AP) axis polarization (Houart et al., 2002; Ohkubo et al., 2002; Shimogori et al., 2004; Niehrs, 2006) (schematized in Fig. 1A,Aa). Therefore, through early Wnt signaling inhibition, we expected to bias cells towards a rostro-ventral pallidal fate. The use of Wnt-inhibitory molecules such as Dkk1 has been previously proposed for the derivation of telencephalic and optic progenitors during mouse and human ESC differentiation (Watanabe et al., 2005; Lamba et al., 2006). Using a modification of our previously published protocol for the generation of cINs (Fig. 1B) (Maroof et al., 2010), we found that, in lieu of Dkk1, adding the tankyrase inhibitor XAV939 (Huang et al., 2009) from differentiation day (DD) 0-5 greatly enhanced the generation of pallidal telencephalic progenitors, as evidenced by

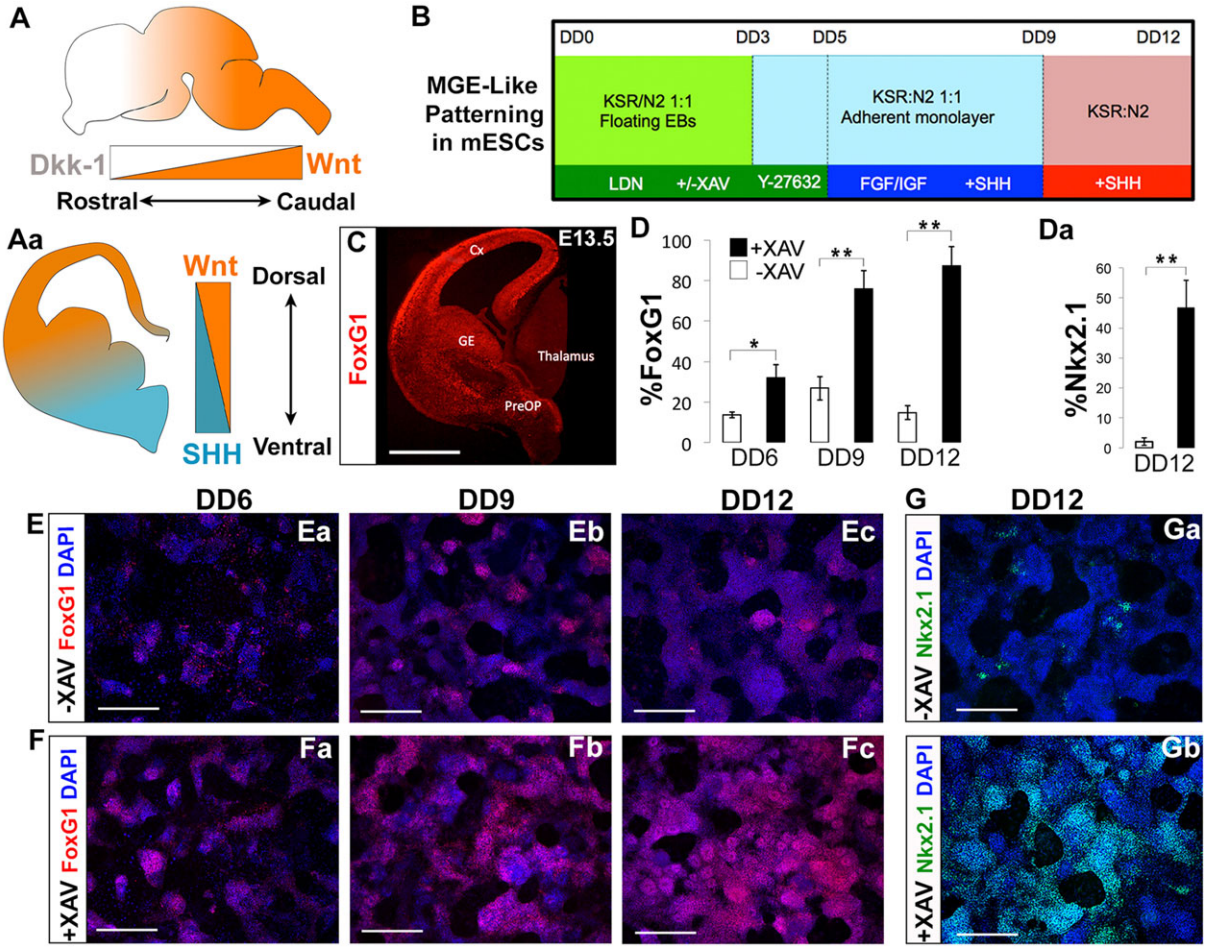

Fig. 1. Early Wnt inhibition efficiently generates mESC-derived ventral telencephalic precursors. (A,Aa) Wnt and Shh signaling schematized in a developing mouse brain. (B) Differentiation paradigm to drive mESCs towards a ventral telencephalic, MGE-like fate, using XAV to inhibit Wnt signaling in combination with LDN, a Bmp inhibitor. (C) Foxg1 immunofluorescence (red) on a coronal hemisection of wild-type E13.5 mouse. Foxg1 (D) and Nkx2.1 (Da) induction are significantly enhanced under the +XAV condition. (E,F) Foxg1 immunofluorescence (red) on mESCs differentiated using protocol (1B) from DD6-DD12, –XAV (top panels) and +XAV (bottom panels). (G,Ga) Nkx2.1 immunofluorescence (green) on mESCs differentiated using protocol (1B) at DD12, –XAV (top panel) and +XAV (bottom panel). (E-Gb) Blue signal shows nuclei labeled with DAPI. Error bars indicate mean values from three independent experiments±s.d. (D,Da; **P*<0.05, ***P*<0.01, Student's *t*-test). Scale bars: 500 µm. DD, differentiation day; E, embryonic day.

Development (2015) 142, 1267-1278 doi:10.1242/dev.111526

Foxg1 and Nkx2.1 expression (Fig. 1C, quantified in Fig. 1D,Da). Foxg1$^+$ cells appeared as early as DD6 (Fig. 1Ea,Fa; 13.7±1.5% −XAV versus 32.0±6.5% +XAV, P=0.03). By DD9, Foxg1 expression increased in rosette-like clusters that began to form (26.8±5.9% −XAV versus 75.9±9.0% +XAV, P=0.002; Fig. 1Eb,Fb). Foxg1 expression peaked at DD12 in our +XAV condition, when neural rosettes comprise the majority of the culture dish (Fig. 1Ec,Fc, quantified in Fig. 1D; 14.8±3.4% −XAV versus 87.3±9.6% +XAV P=0.002). By DD12, XAV-treated differentiations resulted in a 20-fold increase in Nkx2.1 labeling (Fig. 1G; 2.1±1.2% −XAV versus 46.7±9.1% + XAV). XAV treatment also greatly increased the production of Tuj1 (Tubb3 – Mouse Genome Informatics)-expressing neurons (supplementary material Fig. S2).

A dual-reporter mESC line for the isolation of interneuron-fated cells at the progenitor and post-mitotic stages

Previously, we demonstrated that a mESC line modified to express GFP under control of the Lhx6-containing bacterial artificial chromosome (BAC) could be used to isolate putative interneuron precursors, and to identify the two main subclasses of MGE-derived interneurons post transplantation. These included the PV- and SST-expressing subgroups, which were further characterized with electrophysiology, including the presence of 'fast-spiking' action potential trains in the PV-expressing interneurons and non-fast-spiking trains in the SST interneurons (Maroof et al., 2010). To add the capacity of isolating interneuron progenitors, this line was modified with an additional BAC in which mCherry expression is driven by the Nkx2.1 gene (Fig. 2A,B; see Materials and Methods). Of note, the same BAC has previously been used to drive Cre recombinase in Nkx2.1-expression domains of transgenic mice, although Cre-expression was weak within Nkx2.1-expressing cells of the dorsal-most proportion of the MGE (Xu et al., 2008).

In the telencephalon, Nkx2.1 is expressed in the proliferative zones of the MGE and preoptic area, and is downregulated in migratory cINs after cell cycle exit, but persists in striatal interneurons and in PV$^+$ projection neurons of the globus pallidus (Marin et al., 2000; Flandin et al., 2010). Both the induction and the maintenance of Nkx2.1 expression in MGE progenitors are normally dependent on Shh signaling (Fuccillo et al., 2004; Xu et al., 2005). In contrast, Lhx6 is stably expressed in essentially all MGE-derived GABAergic interneurons from the time of cell cycle exit into adulthood (Lavdas et al., 1999; Fogarty et al., 2007). Fluorescence *in situ* hybridization (FISH) analysis revealed a single integration site of the Nkx2.1::mCherry BAC in chromosome 4 (supplementary material Fig. S1A). Additionally, the line primarily used in this analysis, JQ27, formed morphologically typical ESC colonies when plated onto mouse embryonic fibroblasts (MEFs) and standard embryoid bodies (EBs) when floated on a non-adherent substrate (supplementary material Fig. S1B,C). At DD12, all mCherry$^+$ cells differentiated from this line co-express Nkx2.1 (Fig. 2C), although some Nkx2.1$^+$ cells are not mCherry expressing. As expected, a subset of differentiating cells express both Lhx6::GFP and Nkx2.1::mCherry (Fig. 2D). Also as expected, DD12 FACS-isolated Nkx2.1::mCherry-expressing cells, replated onto matrigel in differentiation medium (Neurobasal/B27), strongly express Lhx6::GFP within 24-36 h (supplementary material Movie 1).

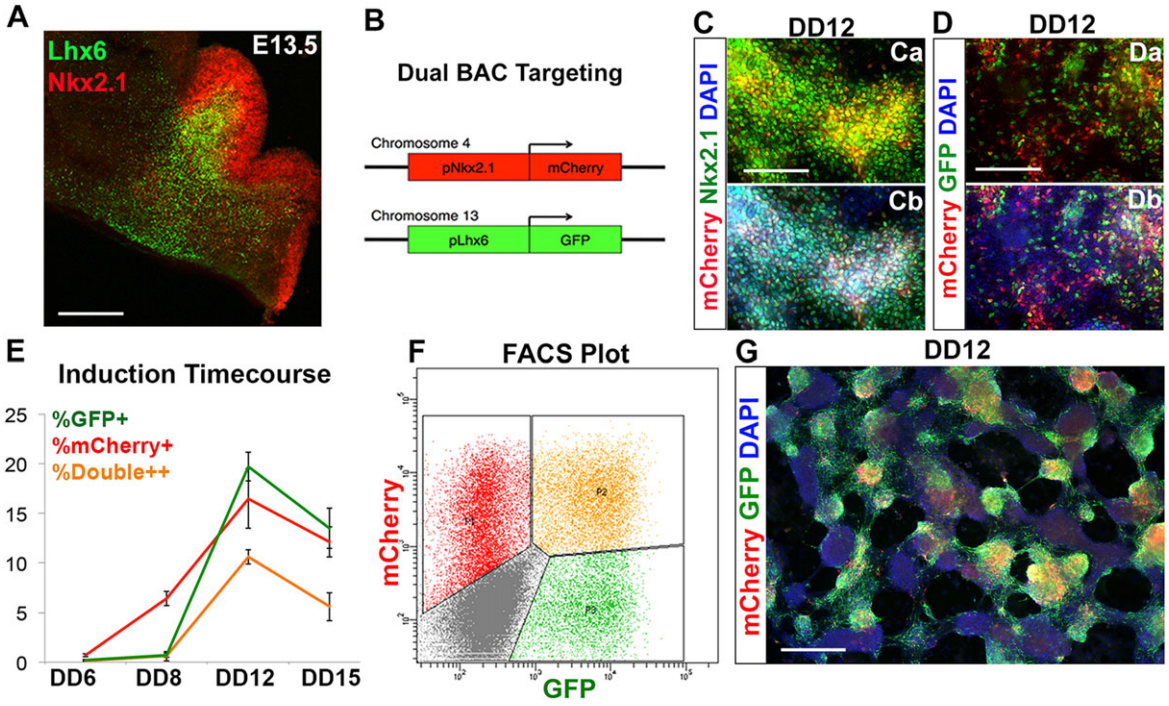

Fig. 2. Generating a dual Nkx2.1::mCherry-Lhx6::GFP BAC reporter mESC line. (A) Lhx6 (green) and Nkx2.1 (red) immunofluorescence on a coronal hemisection of E13.5 medial ganglionic eminence. (B) Schematic of dual BAC integration. An mNkx2.1-mCherry-modified BAC was introduced into the J14 line (Maroof et al., 2010) to generate the Nkx2.1::mCherry-Lhx6::GFP line (JQ27). (C-G) JQ27 mESCs were differentiated via the protocol shown in Fig. 1B. (Ca,Cb) Nkx2.1 (green) and mCherry (red) immunofluorescence on JQ27 mESCs on DD12. (Da,Db) Lhx6::GFP (green) and Nkx2.1::mCherry (red) immunofluorescence on JQ27 mESCs on DD12. (E) Induction of reporters based on FACS; red, total mCherry$^+$ cells (including double-labeled cells); green, total GFP$^+$ cells (including double-labeled cells); orange, double-positive cells. (F) Representative FACS plot of the JQ27 line at DD12 shows mCherry and GFP populations segregating from the autofluorescent background (red, mCherry single$^+$; orange, double$^+$; green, GFP single$^+$; gray, triple-negative). (G) Nkx2.1::mCherry (red) and Lhx6::GFP (green) immunofluorescence on JQ27 mESCs at DD12. Error bars indicate mean values from three independent experiments±s.d. DD, differentiation day; E, embryonic day. Scale bars: 300 µm in A; 150 µm in C,D; 400 µm in G.

Development (2015) 142, 1267-1278 doi:10.1242/dev.111526

Using the protocol described in Fig. 1B, we determined the time course of expression of Nkx2.1 protein along with Nkx2.1::mCherry and Lhx6::GFP. EBs were dissociated and plated onto an adherent substrate as a low-density monolayer on DD3 (100,000 cells/ml). A few Nkx2.1::mCherry$^+$ cells appeared scattered throughout the culture on DD6 (0.7±0.2%); this percentage increased by DD8 (6.4±0.7%) and peaked at DD12 (16.5±3.9%; Fig. 2E). Lhx6::GFP expression was barely detectable at DD6 (0.2±0.1%), nominally increased by DD8 (0.7±0.2%), then peaked at DD12 (19.7±2.0%), before decreasing as a percentage of all cells at DD15 (13.5±3.1%). A representative FACS plot at DD12 is shown, in which three distinct populations segregate from the autofluorescent background: mCherry single-positive, GFP single-positive and mCherry+GFP-double-positive cells (Fig. 2F). Immunofluorescence analysis of mCherry and GFP confirms the FACS-based reporter induction data (Fig. 2G; supplementary material Fig. S3). Consistent with the increased production of pallidal telencephalic progenitors (Foxg1- and Nkx2.1-expressing; Fig. 1), 10 µM XAV939 from DD0-5 increased Lhx6::GFP expression over control (no XAV treatment) 15-fold at DD12 (1.3±0.9% versus 19.7±2.0%, P=0.006) (supplementary material Fig. S4A,C). Maximal results were obtained from Wnt inhibition at the very start of the differentiation protocol, as limiting 10 µM XAV939 to DD3-5 yielded a much smaller increase in Lhx6::GFP (2.9±0.9% versus 19.7±2.0%, P=0.004) (supplementary material Fig. S4B). Taken together, the temporal progression of Foxg1, Nkx2.1 and Lhx6 expression in the ESC differentiation recapitulates expression of these proteins *in vivo* from embryonic day 9 through 15.

Nkx2.1::mCherry and Lhx6::GFP cells exhibit cIN-like neurochemical properties upon transplantation

To characterize the fate potential of either Nkx2.1::mCherry single-positive, mCherry+GFP double-positive, or Lhx6::GFP single-positive cells, JQ27 mESCs were differentiated through DD12, collected via FACS and transplanted into the cortical plate of neonatal mice (schematized in Fig. 3A). Consistent with live-imaging results *in vitro* (supplementary material Movie 1), many of the transplanted mCherry$^+$ cells upregulate Lhx6::GFP upon maturation and integration in the host cortex. At 4 weeks post transplantation, many cells expressing GFP are present from all three isolated fluorescent populations, in a highly dispersed pattern, and form multipolar, aspiny (smooth) morphologies, suggestive of MGE-derived interneuron subgroups (Fig. 3B,Ba). As expected for a reporter driven by promoter elements of Nkx2.1, which is downregulated in cINs shortly after cell cycle exit (Marin et al., 2000), neither Nkx2.1 protein nor mCherry is detected in transplants of cells FACS-isolated for this reporter (Fig. 3C,Ca; supplementary material Fig. S6).

Lhx6::GFP$^+$ cells from mCherry- and GFP-sorted cell transplants gave rise to cells that predominantly express GABA (GFP-sorted cells: 203/224 from four transplants; 89.5±7.0%, and mCherry-sorted cells 104/127 from three transplants; 86.3±5.5%, P>0.2; Fig. 3D,F). In addition, most GFP$^+$ cells from both groups express the MGE-derived cIN marker Sox6 (Azim et al., 2009; Batista-Brito

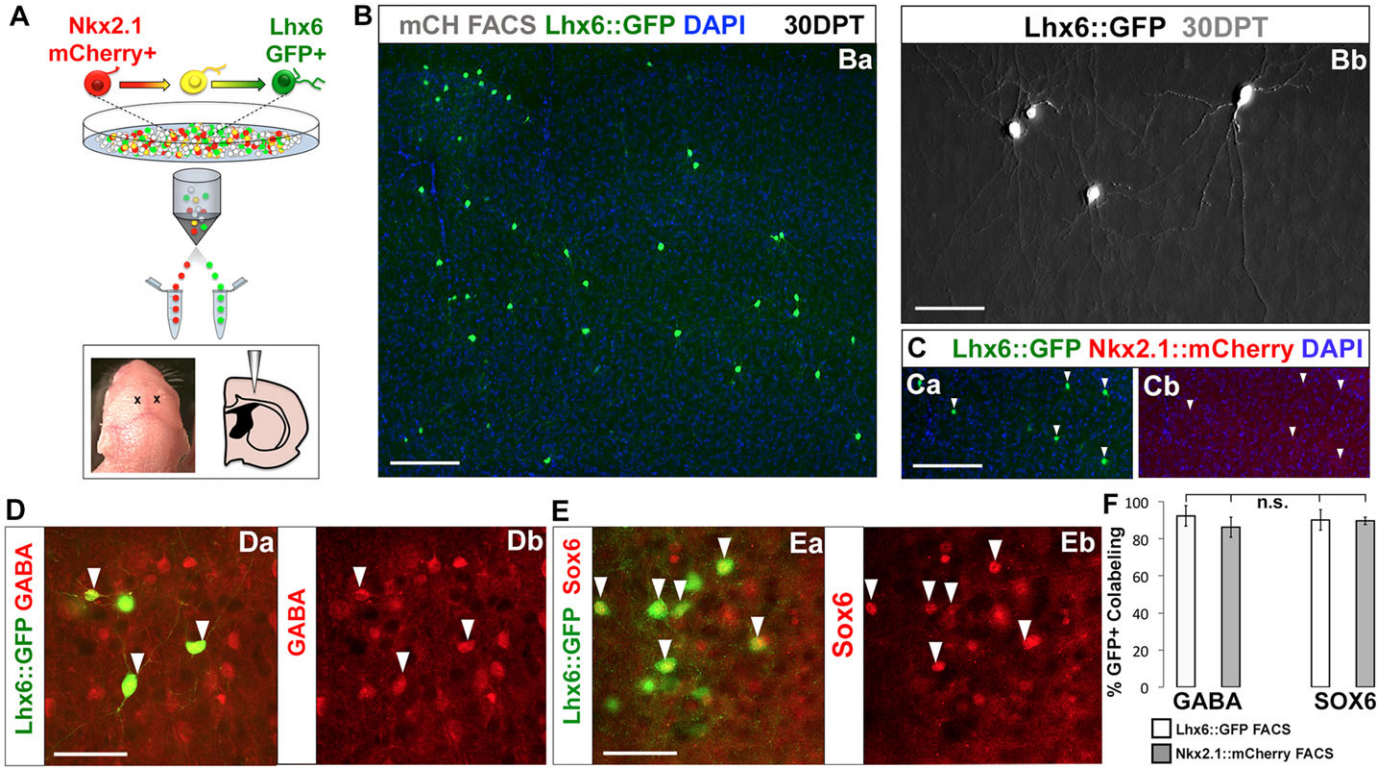

Fig. 3. Maturation of Nkx2.1::mCherry-Lhx6::GFP mESCs into MGE-like Sox6$^+$ GABAergic interneurons. (A) Schematic of reporter progression in mESCs differentiated towards Nkx2.1- and Lhx6-expressing fates (Fig. 1B), then subjected to FACS for mCherry or GFP on DD12, followed by transplantation into neonatal mouse cortex. (B) Representative image of Lhx6::GFP (green) immunofluorescence on a coronal section of somatosensory cortex 30 DPT. This example was obtained from transplantation of a mCherry$^+$, GFP$^-$ population. (Ba) Representative Lhx6::GFP immunofluorescence, showing processes typical of cINs. (C) Representative Lhx6::GFP (green), Nkx2.1::mCherry (red) and the DAPI-stained nuclear (blue) immunofluorescence on a coronal section showing loss of mCherry. (Da,Db) Immunofluorescence of GABA (red) and Lhx6::GFP (green). (Ea,Eb) Representative immunofluorescence of Sox6 (red) and Lhx6::GFP (green). Arrowheads in C-E indicate co-labeled cells. (F) Quantification of Lhx6::GFP co-labeling with GABA and Sox6, from transplants of Lhx6::GFP$^+$ cells (white bars) or Nkx2.1::mCherry$^+$ cells (gray bars). Error bars indicate mean±s.d. from four independent experiments. Scale bars: 200 µm in Ba,C; 50 µm in Bb,D,E.

Development (2015) 142, 1267-1278 doi:10.1242/dev.111526

et al., 2009) (GFP-sorted cells: 122/150 from four transplants; 82.7±8.9%, and mCherry-sorted cells: 115/127 from three transplants; 89.7±2.1%, $P>0.9$, Fig. 3E,F). Together with evidence that the vast majority of cells express the telencephalic marker Foxg1 at transplantation (supplementary material Fig. S5; mCherry/Foxg1: 93.4±0.82% and GFP/Foxg1: 98±0.63%), these results suggest that Lhx6::GFP-expressing cells identified in transplant cells sorted for Lhx6::GFP or Nkx2.1::mCherry predominantly represent cINs.

Recapitulating developmental programs *in vitro* yields differentially enriched populations of PV versus SST-fated mESC-derived cINs

Although a detailed understanding of the molecular bases for cIN subgroup specification is not known, for the MGE-derived SST- or PV-expressing subgroups several factors influence their fate determination. First, whereas, within a given cortical layer, PV- and SST-expressing interneurons have similar birthdates (Cavanagh and Parnavelas, 1988; Rymar and Sadikot, 2007), the predominance of PV over SST subgroups in the later-born, superficial cortical layers corresponds to a larger percentage of all SST interneurons being generated earlier than all PV interneurons (Butt et al., 2005; Xu et al., 2010b). Second, higher levels of signaling for the morphogen Shh in dorsal MGE appears to bias those Nkx2.1-expressing progenitors to generate SST-expressing interneurons (Xu et al., 2005, 2010a; Wonders et al., 2008) (schematized in Fig. 4A).

To determine whether Shh signaling influences interneuron fate in the mESC system, we first sought to direct mESCs towards either

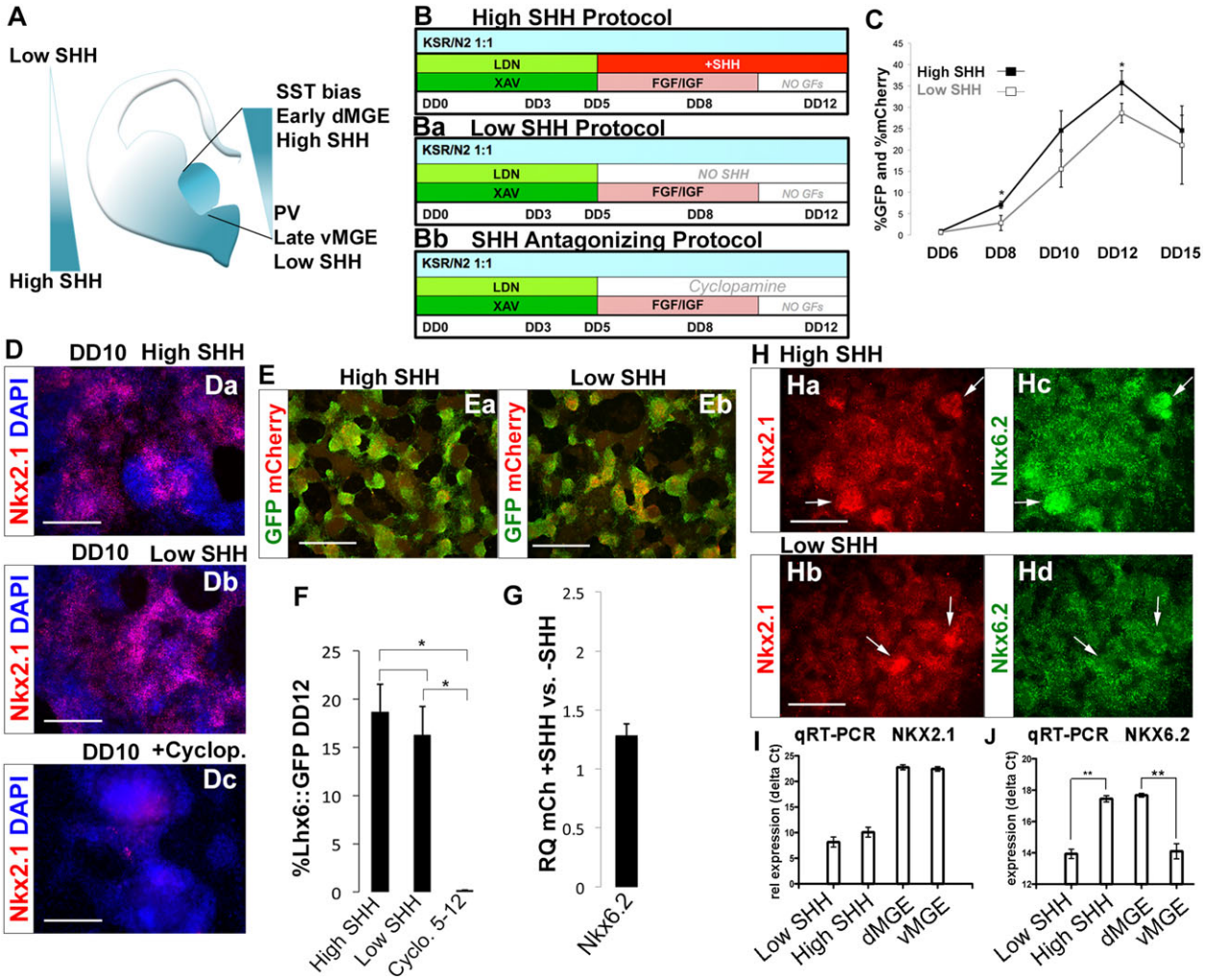

Fig. 4. Induction of dorsal MGE-like patterning at higher levels of exogenous Shh. (A) Schematics of Shh signaling strength in the embryonic telencephalon. (B-Bb) Shh manipulations during differentiation. (B) Shh (50 ng/ml) from DD5-12. (Ba) No Shh added. (Bb) Cyclopamine (5 µM) from DD5-12. (C) FACS quantification of Lhx6::GFP and Nkx2.1::mCherry induction. Black and gray lines indicate the added or not added Shh conditions, respectively. Based on the effects of cyclopamine (below), these conditions are termed 'high' and 'low' Shh, respectively. (D) Nkx2.1 (red) immunofluorescence on DD10. High and low Shh conditions (Da,Db) are similar, whereas cyclopamine (Dc) nearly eliminates Nkx2.1 expression. (E) GFP (green) and mCherry (red) immunofluorescence at DD12 showing similar induction levels between the two Shh levels (B versus Ba). (F) Lhx6::GFP induction by FACS on DD12, high and low Shh conditions are not statistically different, whereas cyclopamine (see Bb) nearly eliminates Lhx6::GFP expression. (G) Relative expression of Nkx6.2 RNA transcripts in mCherry-sorted cells at DD10, showing increased expression in response to Shh (50 ng/ml); 1=RQ mCherry with no Shh. (H) Nkx2.1 (red) and Nkx6.2 (green) immunofluorescence on DD12 revealed that high Shh induced Nkx6.2 in cell clusters that also express Nkx2.1 (arrows in Ha,Hc). Low Shh produced little co-expression of Nkx6.2 in Nkx2.1-expressing cell clusters (arrows in Hb,Hd). (I) qRT-PCR for Nkx2.1 mRNA expression levels revealed no significant difference between the high and low Shh protocols nor between E13.5 dorsal or ventral MGE. (J) qRT-PCR for Nkx6.2 mRNA revealed significant differences in Nkx6.2 expression across high and low Shh protocols, which mirror levels in dorsal versus ventral MGE. Error bars indicate mean values from three independent experiments±s.d., $^{**}P<0.01$ $^{*}P<0.05$, Student's *t*-test. Scale bars: 200 µm in Da-Dc; 400 µm in Ea,Eb,Ha,Hb.

Development (2015) 142, 1267-1278 doi:10.1242/dev.111526

a dorsal or ventral MGE-like fate by providing higher or lower levels of Shh signaling during differentiation (Fig. 4A,B-Bb). As shown above, cultures exposed to 50 nM Shh from DD5-12 produced many Nkx2.1- and Lhx6-expressing cells, but we were initially surprised to find that, in the absence of exogenous Shh (but after exposure to XAV), there was only a moderate reduction in numbers of these cells (Fig. 4B-F). Addition of the Shh signaling antagonist cyclopamine to the no-exogenous Shh condition dramatically reduced both Nkx2.1 and Lhx6::GFP induction (Fig. 4Bb,Dc,F). As Shh signaling is required for both the induction and the maintenance of Nkx2.1 expression (Fuccillo et al., 2004; Xu et al., 2005), this result indicates that the no-exogenous Shh condition contains endogenous Shh signaling. We thus designate it as a 'low-Shh' condition in contrast to the 'high Shh' signaling condition produced by addition of Shh. Importantly, Nkx2.1::mCherry cells exposed to the high Shh condition have increased co-localization with Nkx6.2 relative to the low Shh condition (Fig. 4H; quantified by RT-PCR in Fig. 4G). As our previous studies have demonstrated that the higher levels of Shh signaling induce Nkx6.2 in the dorsal MGE relative to ventral MGE (Xu et al., 2005, 2010a), and, as the relative levels of Nkx2.1 and Nkx6.2 transcript are similar in high versus low Shh-exposed cultures as they are in dorsal versus ventral MGE cells (Fig. 4I,J), Nkx2.1::mCherry^{+} cells in our high and low Shh protocols have features of dorsal versus ventral MGE, respectively.

Based on the temporal and spatial/Shh signaling influence on SST versus PV fate determination *in vivo*, we next sought to determine whether manipulations of these factors can enrich for SST- versus PV-expressing interneuronal fates. To confirm that differential exposure to Shh alone could influence interneuron fate determination, we compared transplants of Lhx6::GFP-expressing cells at DD14 that were exposed to either the high or the low Shh conditions (Fig. 5A-E). As the high Shh condition enriches for Nkx6.2, which *in vivo* is enriched in the dorsal MGE in progenitors of SST-expressing interneurons (Fogarty et al., 2007; Sousa et al., 2009), as well as in the preoptic area, where they give rise to Lhx6^{-} interneuron progeny (Gelman et al., 2009), we predicted that high Shh would enhance the generation of the SST-expressing subgroup (Fig. 5C-Db). Indeed, high Shh levels resulted in a strong bias for more Lhx6::GFP^{+} cells to become SST- than PV-expressing (Fig. 5E; 55/82, 67.1±1.9% SST, versus 9/82, 11.1±3.9% PV; n=3 brains, P<0.001). In the low Shh condition, GFP^{+} cells were more than twice as likely to differentiate into PV-expressing interneurons, whereas the percentage of cells differentiating into SST-expressing interneurons was greatly reduced (Fig. 5E; 18/79 cells, 25.9±6.8% GFP/PV, versus 30/79, 40±4.4% GFP/SST; n=3 brains, P<0.05).

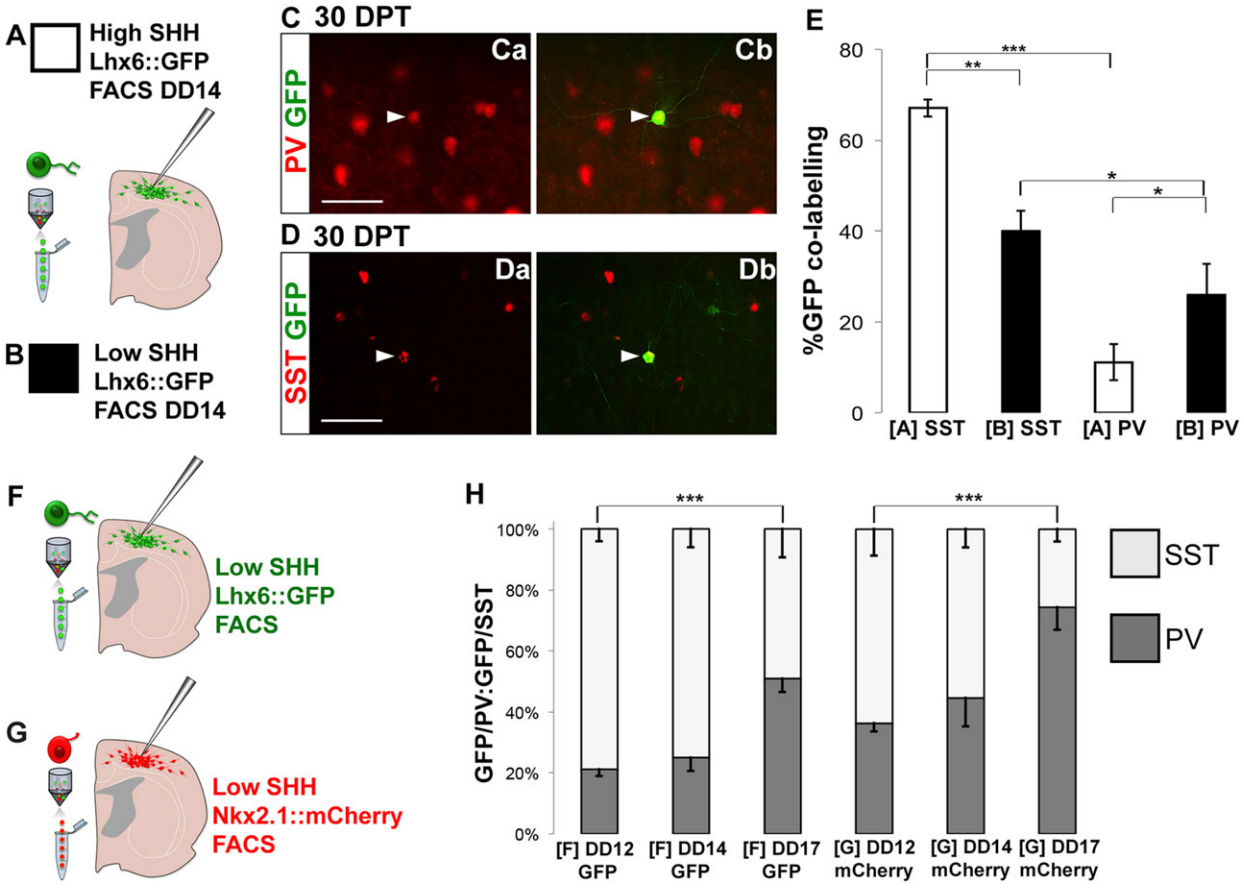

Fig. 5. Shh manipulation and birthdate influences PV versus SST fate profiles in transplanted mESCs. (A,B) Schematic of the high (+50 ng/ml Shh, DD5-12; A) and low (no exogenous Shh; B) Shh protocols. DD14 cells were sorted for Lhx6::GFP and then transplanted into the neonatal cortex. (Ca,Cb) PV (red) and GFP (green) immunofluorescence. Arrowheads indicate Lhx6::GFP/PV co-expression. (Da,Db) SST (red) and GFP (green) immunofluorescence. Arrowheads indicate Lhx6::GFP/SST co-expression. (E) Quantification of SST- versus PV-fated Lhx6:GFP-expressing cells in neocortical sections 30 DPT. High Shh resulted in a bias for Lhx6::GFP^{+} neurons to take SST^{+} instead of PV^{+} fates (n=3 brains; ***P<0.001, **P<0.01, *P<0.05, Student's t-test). (F,G) Cells were differentiated without Shh and sorted for either GFP (F, green) or mCherry (G, red) at DD12, 14 or 17. (H) Quantification of SST or PV expression in Lhx6::GFP-expressing cells. The ratio of PV:SST increases over time in culture in both mCherry^{+} and GFP^{+} FACS-isolated cells. (n=3 brains; ***P<0.0001, one-way ANOVA). Scale bars: 50 µm. DD, differentiation day; PV, parvalbumin; SST, somatostatin.

Development (2015) 142, 1267-1278 doi:10.1242/dev.111526

Although these results support our previous evidence that Shh signaling promotes SST over PV fates (Xu et al., 2010a), the yield of PV^+ interneurons remained relatively low even in the low Shh condition. To determine whether time in culture can also be used to manipulate fates, we employed two approaches. First, we collected cells at different times. As later collections of GFP^+ cells would contain a mix of cells born from around DD8 onwards, we also collected cells based on expression of mCherry. Although mCherry protein is likely to perdure transiently in post-mitotic cells after downregulation of Nkx2.1, at any time in culture the mCherry population that is fated to become Lhx6-GFP^+ interneurons, and thus be visible in our transplantation assay, will tend to be younger than the GFP^+ population. Our live imaging is consistent with this paradigm, as the Nkx2.1::Cherry signal decreases over a 36-h period, whereas Lhx6::GFP signal becomes stronger (supplementary material Movie 1). To compare effects of time in culture and maturational state (i.e. Nkx2.1::mCherry versus Lhx6::GFP) on interneuron fates in our system, we compared transplants of GFP- versus mCherry-expressing cells from collections at DD12, 14 and 17 (Fig. 5F-H). Whether cells were collected by expression of GFP or of mCherry [then identified 30 days post transplant (DPT) by GFP expression], there was a significant effect of age of culture at collection on the ratio of PV- versus SST-expressing cells [GFP: PV/SST at DD12, 14, 17; $F(2,6)=101.53$, $f_{crit}=8.05$, $P<0.0001$. mCherry: PV/SST at DD12, 14, 17; $F(2,13)=29.2$, $f_{crit}=5.36$, $P<0.0001$]. There was also a significant effect of collection of mCherry versus SST, as, at each age, more $mCherry^+$ cells gave rise to PV and fewer gave rise to SST than did GFP^+ cells collected at that age (Fig. 5G,H; sorted GFP^+ cells: 16.4±1.8% PV and 60.6±3.0% SST at DD12, 19.6±3.53% PV and 58.0±4.6% SST at DD14, 34.7±3.1% at DD17; sorted $mCherry^+$ cells: 26.6±2.0% PV and 46.8±6.4% SST at DD12, 33.8±7.1% PV and 42±4.6% SST at DD14, 55.45±5.6% PV and 19.1±3.1% SST at DD17; $P<0.05$ at all time points).

To maximally enrich differentiations for PV- versus SST-fated cells, neonatal pups were transplanted with high-Shh protocol, Lhx6::GFP FACS-isolated cells on DD12 (Fig. 6A), or with low-Shh protocol, Nkx2.1::mCherry-expressing cells on DD17 (Fig. 6B). Lhx6::GFP^+ cells in neocortical tissue sections were examined at 30 DPT. Transplants of the high-Shh, DD12 GFP-sorted cells were highly enriched for SST-expressing relative to PV-expressing interneurons (440/697 SST^+/GFP^+ cells, 63.9±8.2% versus 79/697 PV^+/GFP^+, 10.36±4.2% PV; $n=3$ differentiations, 9 transplanted brains, $P<0.001$; Fig. 6Aa-Ae). In marked contrast, transplants of the low-Shh, DD17 mCherry-sorted cells were highly enriched for PV-expressing interneurons (PV^+/GFP^+ 279/498, 55.5±5.6% PV versus 73/498 SST^+/GFP^+, 19.1±3.0% SST; $n=4$ differentiations, 11 brains total, $P<0.001$; Fig. 6Ba-Bd,Ae). Both protocols yielded ~25% Lhx6::GFP^+ cells expressing neither PV nor SST (Fig. 6Ae,Be), consistent with our previous observations (Maroof et al., 2010; Petros et al., 2013). These PV^- and SST^- cells generally expressed GABA, but did not co-label for markers of other interneuron subgroups, such as calretinin, calbindin, reelin or neuropeptide Y (Npy) (data not shown).

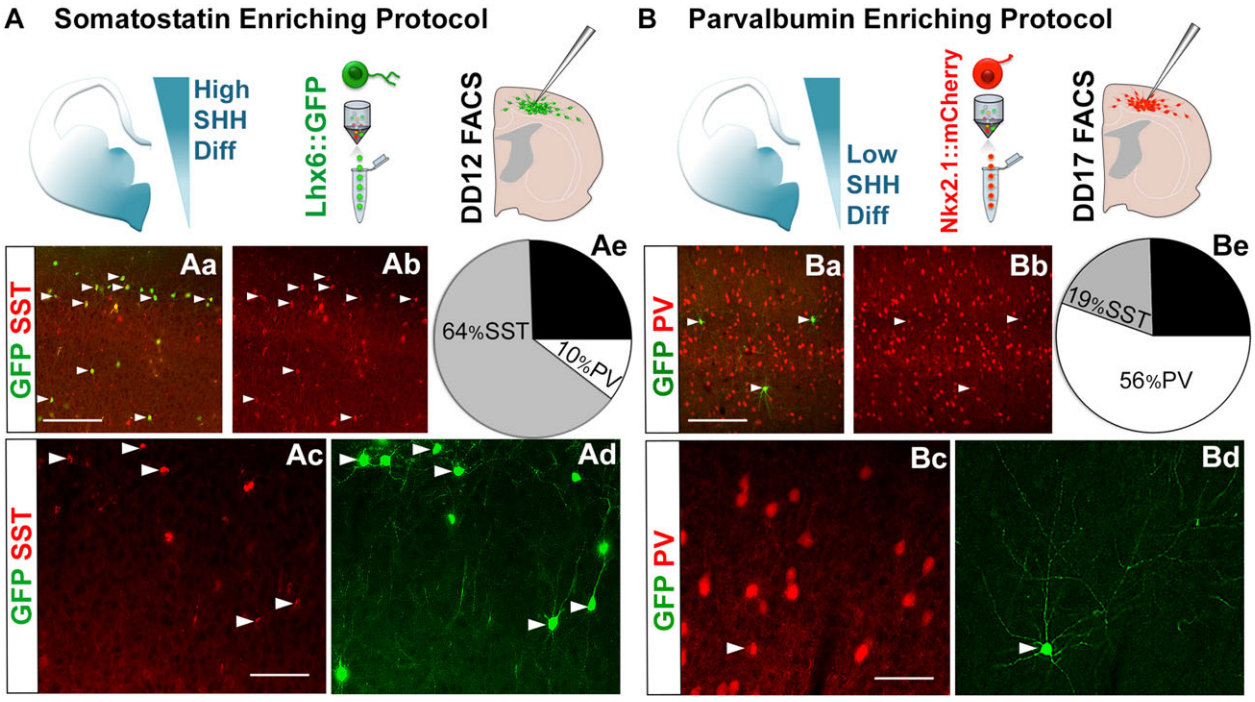

Fig. 6. Manipulations of time in culture and Shh exposure differentially enrich for PV- versus SST-fated mESC-derived cINs. (A) In the SST-enriching protocol, cells were differentiated with Shh; then, Lhx6::GFP^+ cells were sorted at DD12 and transplanted into neonatal cortex. (Aa,Ab) SST (red) and GFP (green) immunofluorescence on cortical sections at 30 DPT. Arrowheads indicate GFP-expressing cells that co-label with SST. (Ac,Ad) SST (red) and GFP (green) immunofluorescence, showing multipolar interneuron-like morphologies; arrowheads indicate Lhx6::GFP/SST co-expression. (Ae) Quantification of SST or PV co-labeling with GFP (63.9±8.2% SST and 10.36±4.2% PV; $n=3$ independent differentiations, 9 brains total; $P<0.001$). (B) In the PV-enriching protocol, cells were differentiated without exogenous Shh, and Nkx2.1::$mCherry^+$ cells were sorted at DD17. (Ba,Bb) PV (red) and GFP (green) immunofluorescence on 30 DPT cortex. Arrowheads indicate GFP-expressing cells that co-label with PV. (Bc,Bd) PV (red) and GFP (green) immunofluorescence, showing cells with a multipolar morphology; arrowheads indicate Lhx6::GFP/PV co-expression. (Be) Quantification of SST or PV co-labeling with GFP (55.5±5.6% PV and 19.1±3.0% SST; $n=4$ independent differentiations, 11 brains total; $P<0.001$). Interprotocol differences in PV versus SST co-labeling with GFP are significant, $P<0.001$. DD, differentiation day; PV, parvalbumin; SST, somatostatin. Scale bars: 100 µm in Aa,Ba; 50 µm in Ac,Bc.

Development (2015) 142, 1267-1278 doi:10.1242/dev.111526

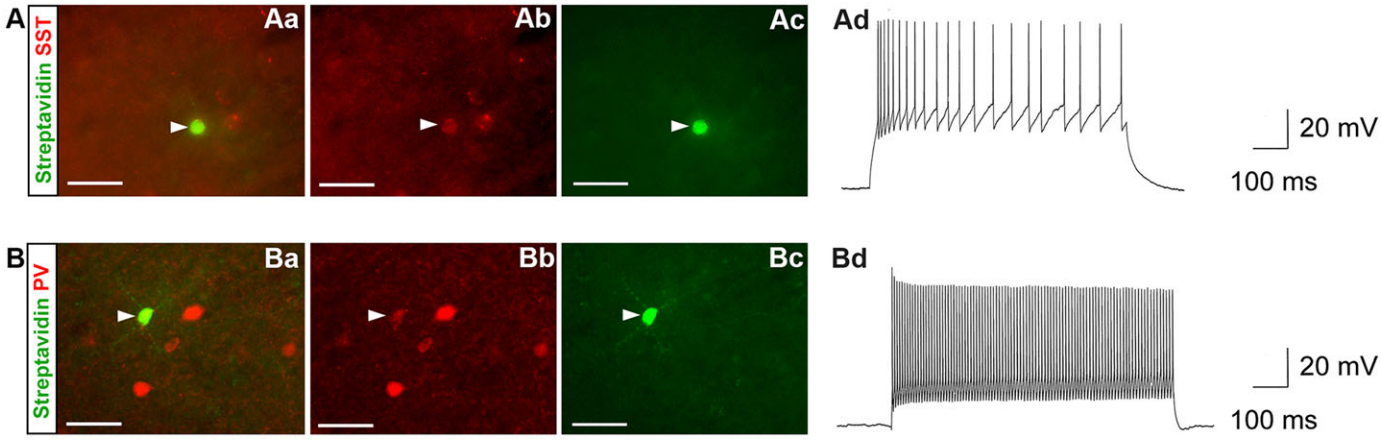

Fig. 7. JQ27-derived, Lhx6-GFP cells exhibit electrophysiological characteristics of cINs. 60-70 DPT, 275-µm-thick neocortical slices were subjected to whole-cell patch-clamp recordings and fluorescence labeling. (Aa-Ac) Neurobiotin-streptavidin-Alexa Fluor (green) and SST (red) immunofluorescence. (Ba-Bc) Neurobiotin-streptavidin-Alexa Fluor (green) and PV (red) immunofluorescence. (Ad,Bd) Electrophysiological responses of two transplanted cells. These cells were tested for threshold (Ad,Bd) response to a depolarizing current injection of 20 mV. The cell in A co-labels for GFP (not shown), SST (Ab; red) and NB (Ac; green), and exhibited an adapting, non-fast-spiking pattern and fast-spiking discharge pattern (Ad) typical of many SST-expressing interneurons. The cell in B-Bc co-labels for GFP (not shown), PV (Ba) and NB (Bb) and exhibited a fast-spiking discharge pattern (Bd) typical of PV-expressing interneurons. Scale bars: 40 µm.

Transplanted JQ27-derived cINs have MGE-interneuron-like spiking characteristics

The fate-related data described herein strongly suggest that, as we found with the Lhx6-GFP parent line (J14; Maroof et al., 2010), JQ27-derived cells can differentiate into neurons that exhibit features of MGE-derived cIN subgroups *in vivo*. To test this directly, we examined the biophysical properties and the functional incorporation of transplanted Nkx2.1:mCherry cells that had been differentiated as described for Fig. 4B. Whole-cell patch-clamp recordings were performed on GFP^+ cells in acutely prepared cortical slices between 60 and 70 DPT (Fig. 7). We recorded a total of 14 GFP^+ cells across nine brains (Table 1) and found that GFP^+ cells could be characterized into two physiologically distinct populations. Non-fast-spiking (NFS) patterns frequently correlate with SST expression, whereas cells exhibiting fast-spiking (FS) firing patterns are typical of the PV-expressing interneurons (Kawaguchi and Kubota, 1996). As predicted, we observed both SST^+ NFS patterns (accommodating, average AP 1/2 width 0.84±0.09 ms, Fig. 7A-Ac) and PV^+ FS patterns (non-accommodating, average AP 1/2 width 0.48±0.03 ms, Fig. 7B-Bc). Average resting membrane potentials (RMPs) were similar for both FS and NFS cells and typical of endogenous mature cINs (−70.7±5.8 mV and −66.3±5.1 mV, respectively).

DISCUSSION

This study aimed to accomplish three objectives: (1) to increase the efficiency of generating ventral telencephalic mESC-derived neurons; (2) to generate a dual-reporter mESC line that enables the isolation of MGE-like cIN progenitors ($Nkx2.1^+$), as well as their cIN progeny ($Lhx6^+$); and (3) to generate highly enriched populations of either PV- or SST-fated precursors by recapitulating developmental programs *in vitro*. Progress in each of these endeavors provides a robust system for the study of cIN fate determination, along with the ability to generate large numbers of selectively fated PV versus SST interneuron precursors for transplantation studies.

Table 1. Comparison of GFP^+ cell populations: non-fast spiking cells (NFS; top row) and fast-spiking non-adapting cells (FS; bottom row)

Age	Electrophysiological profile	Number of cells	Average RMP (mV ±s.d.)	Average AP 1/2 width (ms ±s.d.)
60-70 DPT	NFS	8	–66.3±5.1	0.84±0.09
60-70 DPT	FS	6	–70.7±5.8	0.48±0.3

AP, anterior-posterior; RMP, resting membrane potential.

These findings build upon previous reports that Wnt signaling inhibition with Dkk1 during the initial phase of stem cell differentiation potentiates expression of the telencephalic marker Foxg1 (Watanabe et al., 2005; Danjo et al., 2011). We find that Wnt signaling inhibition by the small molecule XAV939 greatly increases the efficiency of generating ventral telencephalic patterning in mESCs, as we achieve a near 100% differentiation to $Foxg1^+$ progenitors (Fig. 1). Dkk1 acts through binding to the Wnt co-receptor Lrp6 (Mao et al., 2001). By contrast, XAV939 inhibits Wnt signaling by inhibiting tankyrase, resulting in increased cytosolic axin and enhanced degradation of β-catenin (Huang et al., 2009; Fancy et al., 2011). In human ESC differentiation, XAV939 treatment also significantly increases Foxg1 induction relative to Dkk1 (Maroof et al., 2013). This increase in induction efficiency for Foxg1 suggests that XAV939 is probably more stable or more potent in inhibiting Wnt signaling than recombinant Dkk1.

An additional benefit of XAV939 treatment is that it results in telencephalic differentiation that is heavily ventralized, with many cells expressing Nkx2.1, without the addition of Shh (Fig. 4). However, consistent with previous reports on the requirement of Shh signaling for both the induction and the maintenance of Nkx2.1 (Fuccillo et al., 2004; Xu et al., 2005; Flandin et al., 2011), cyclopamine nearly eliminates this Nkx2.1 expression (Fig. 4). This situation allows us to consider differentiations not exposed to exogenous Shh to be a relatively low Shh condition, compared with those exposed to 50 ng/ml Shh. Importantly, the exogenous-Shh condition induces expression of Nkx6.2 in many Nkx2.1-expressing progenitors (Fig. 4). Nkx6.2 is expressed in the dorsal MGE together with other genes associated with higher levels of Shh signaling, such as Gli1 and Hip1 (Wonders et al., 2008). Nkx6.2 is also enriched in progenitors of SST-expressing interneurons (Fogarty et al., 2007; Sousa et al., 2009), which transplantation experiments have shown to be enriched in the dorsal MGE (Flames et al., 2007; Inan et al., 2012). By using Wnt inhibition early in the

Development (2015) 142, 1267-1278 doi:10.1242/dev.111526

differentiation, together with varying levels of Shh, we have thus created culture conditions that replicate aspects of intra-MGE patterning.

To determine whether the patterning-like effects of Shh on the ESC differentiations matches predicted effects on interneuron fates, we compared the effect of exogenous (for the current discussion 'high') Shh versus no exogenous ('low') Shh on the fates ES differentiations sorted for Lhx6::GFP at DD14. Indeed, the low Shh condition resulted in a significantly higher ratio of PV:SST fates than the high Shh condition (Fig. 5). These results are consistent with Shh signaling playing an instructive role in the differential fate determination of SST versus PV interneurons (Xu et al., 2010a). Of note, it has also been reported that removal of Shh from the MGE mantle reduces both SST and PV interneurons by similar proportions (Flandin et al., 2011). However, as PV interneurons might preferentially originate from MGE subventricular zone (SVZ) divisions that would be closer to the MGE mantle source of Shh (Glickstein et al., 2007; Lodato et al., 2011), the net effect of Shh loss in the MGE mantle on cIN composition is difficult to determine without knowing how Shh signaling itself is altered by this loss within the various populations of MGE progenitors.

Although Shh alteration alone significantly affected the interneuron fates of Lhx6::GFP$^+$ cells transplanted from differentiation of mESCs, the effect was partial. As birthdate has also been associated with differential fates of MGE progenitors, we compared the transplanted fates of collections from various times of differentiation, and also collected cells based on Nkx2.1::mCherry expression. As expected, transplantation of mCherry-expressing cells resulted in plentiful identification of Lhx6::GFP-expressing cells in transplanted neocortex, and none of these cells expressed mCherry or Nkx2.1 (Fig. 3; supplementary material Fig. S6). In addition to the Shh effect noted above, there were significant effects of time and Nkx2.1::mCherry collection on interneuron fate (Fig. 5). In sum, early (differentiation day 12) collection and transplantation of Lhx6-expressing cells from the high Shh condition resulted in a roughly 6:1 ratio of SST to PV interneurons, whereas late (day 17) collection of mCherry-expressing cells from low Shh condition resulted in a roughly 3:1 ratio of PV to SST interneurons (Fig. 6).

Although cells collected based on Nkx2.1::mCherry expression at a given stage and condition give rise to relatively more PV interneurons than do those collected by their Lhx6::GFP expression, it is appropriate to note that maturational stage or birthdate is not likely to be the only determinant of this difference. The Nkx2.1-Cre mouse generated with the same BAC used in this paper had relatively weak expression of Cre in the dorsal-most MGE, and fate mapping of this mouse labeled a modestly higher proportion of neocortical PV interneurons (roughly 80%) than of SST interneurons (roughly 70%) (Xu et al., 2008). It is therefore likely that some of the enrichment for PV fates seen with Nkx2.1::mCherry collections is due to a partial bias for this transgene to express in progenitors of PV versus SST interneurons.

In summary, we demonstrate the ability to isolate enriched populations of differentially fated mESC-derived PV$^+$ or SST$^+$ cIN subgroups at the time of fate conferral. Furthermore, this is the first report of a dual-BAC reporter ESC system employed to isolate differentially fated forebrain subgroups within a common neuronal class, a valuable approach applicable to other lineages of interest. In addition to the implications of this work for identification of genes differentially expressed in the post-mitotic precursors of two major cIN subclasses, it is now possible to use mESCs to explore pre-clinical cell-based therapies for disorders thought to involve specific deficits in these neurons, including epilepsy and schizophrenia.

MATERIALS AND METHODS

Generation of the JQ27 mES-Lhx6::GFP/Nkx2.1::mCherry line

The previously generated J14 *mES-Lhx6::GFP* line (Maroof et al., 2010) was modified with an Nkx2.1::mCherry-containing BAC, using the same BAC (RPCI-23-3H18) used to obtain expression of Cre in Nkx2.1-expressing cells in transgenic mice (Xu et al., 2008). This BAC was modified such that mCherry replaces most of exon 2 of Nkx2.1 in frame, and a blastocidin resistance cassette was inserted into the BAC backbone for subsequent mammalian selection (Tomishima et al., 2007). This BAC was then electroporated into the mESC line (J14) to generate the Lhx6::GFP/Nkx2.1::mCherry line. Karyotype and FISH analysis revealed a single integration site on chromosome 13 of Lhx6::GFP and a single integration site on chromosome 4 of Nkx2.1::mCherry (supplementary material Fig. S1).

mESC culture

Mouse ESCs were grown on mouse embryonic fibroblasts (MEF CF-1 MITC7M, GSC-6101M, Global Stem) in standard mESC medium {knockout DMEM [Invitrogen], 15% FBS [Invitrogen-Thermo Fisher Scientific], supplemented with L-glutamine, primocin, MEM nonessential amino acids, β-mercaptoethanol and LIF [1.4 µl/ml (10^7 U/ml)] ESG1107, Millipore}. For differentiation, mESCs were treated with 0.05% trypsin and suspended at 70,000 cells/ml (Maroof et al., 2010; Watanabe et al., 2005). Floating embryoid bodies (EBs) were grown in a 1:1 mixture of KSR (10828-028, Invitrogen) and N2 media (DMEM:F12, 11330, Invitrogen; N2 07156, Stemgent) supplemented with LDN-193189 (250 nM, 04-0074, Stemgent) and XAV939 (10 µM, 04-0046, Stemgent). On DD3, EBs were dissociated using accutase (A1110501, Invitrogen) and plated onto poly-L-lysine (P6282, Sigma)- and laminin (L2020, Sigma)-coated plates at 100,000 cells/ml in N2:KSR medium. On DD5, XAV and LDN treatment ceased, and medium was supplemented with FGF-2 (10 ng/ml, DD5-9, 233-FB, R&D Systems), IGF1 (20 ng/ml, day 5-9, 291-G1-200/CF, R&D Systems), with or without Shh (50 ng/ml, Shh-N-C25II, R&D Systems; DD5-12). Medium was changed at DD0, DD3 and every other day until FACS sorting or IHC analysis. Y-27632 (10 nm, Tocris) was added prior to EB dissociation at DD3 and again prior to terminal dissociation and during FACS. Cultures were fixed and analyzed by immunofluorescence or subjected to FACS.

Cell sorting

Cells were treated with accutase (Invitrogen) for 30 min, followed by gentle trituration to dissociate to single cells. The cells were centrifuged at 1000 rpm (250 ***g***) for 5 min, resuspended in DMEM:F12 (11039-021, Invitrogen) with 20% HyClone FBS (Atlanta Biologicals) and Y-27632 (10 nm, 1254, Tocris), then passed twice through a 40-µm filter. The cell suspension was kept on ice until FACS (Aria II, BD Biosciences) and analyzed using FACS Diva software (version 6.1.3).

Gene expression profiling

Total RNA was extracted from day 12 mESC differentiations or E12.5 MGE using an RNeasy kit (Qiagen). For each sample, 1 µg of total RNA was treated for DNA contamination and reverse-transcribed using the Quantitect RT kit (Qiagen). Amplified material was detected using TaqMan probes detecting either Nkx2.1 (Mm00447558_m1) or Nkx6.2 (Mm00807812_g1) and using a PCR kit (Applied Biosystems) on a Mastercycler RealPlex2 (Eppendorf). All results were normalized to a *Gapdh* control gene, with a cut-off at 45 cycles, and Δ_{Ct} values were calculated by comparison to results from RNA samples isolated from undifferentiated ESCs. There were two replicates of three independent samples at each data point.

Neonatal cortical transplantation

Transplantation into the somatosensory neocortex of cooling-anesthetized neonatal pups was conducted as described previously (Maroof et al., 2010; Wonders et al., 2008). Between 20,000 and 40,000 cells were injected into the cortical plate at the following coordinates from bregma (2.0 mm anterior, 2.5 mm lateral, 1.0 mm deep), targeting cortical layers 3-6 of CD1 pups at P0-1. Animal care was in accordance with institutional

Development (2015) 142, 1267-1278 doi:10.1242/dev.111526

guidelines at the Weill Cornell Medical College and The Children's Hospital of Philadelphia.

In vitro immunohistochemistry

Cells were fixed in 4% paraformaldehyde, blocked in BSA/PBST, in some cases pretreated with 1 mM ETDA/PBS (65°C, 5 min), then immunolabeled with antisera: rabbit anti-Lhx6 (1:1000, a gift from V. Pachnis, Division of Molecular Neurobiology, MRC National Institute for Medical Research, London, UK), rabbit anti-Foxg1 (Neuracell; 1:1000), chicken anti-GFP (Abcam, ab13970; 1:1000), mouse anti-Nkx2.1 (Abcam, ab76013; 1:500), rat anti-RFP antibody (Chromtek, 5F8; 1:400), mouse anti-Tuj1 (Promega, G712A; 1:1000), rabbit anti-Nkx6.2 (1:500, a gift from M. Sander, UCSD School of Medicine Department of Pediatrics, Department of Cellular & Molecular Medicine) and nuclear staining with DAPI (Invitrogen, D3971). Secondary antibodies were conjugated to Alexa fluorophores (488, 568 or 680, Invitrogen) or Cy5 (Jackson ImmunoResearch).

In vivo fate quantification

Fixed brains were sectioned in the coronal plane at 50 µm on a vibrating microtome (Leica). Sections including somatosensory cortex were labeled with chicken anti-GFP (Abcam, ab13970; 1:1000) immunofluorescence, rabbit anti-PV (Swant, PV-25; 1:2000), rat anti-SST (Millipore, 14224; 1:2000), rabbit anti-GABA (Sigma-Aldrich, A2052; 1:1000), rabbit anti-Sox6 (Abcam, ab30455; 1:2000), rabbit anti-Npy (Immunostar, 22940; 1:300) or goat anti-choline acetyltransferase (Millipore, AB144P; 1:500) and nuclear staining with DAPI. Secondary antibodies were conjugated to Alexa fluorophores (Invitrogen) or Cy5 (Jackson ImmunoResearch). Generally, 12-15 sections were evaluated per marker. Transplanted animals were excluded if there were fewer than 25 total GFP^+ cells present, and only GFP^+ cells engrafted in cortical layers 2-6 were included in fate analysis. Each condition in which both timing and exposure to exogenous Shh were varied was repeated on at least three separate occasions, with a minimum of two transplanted mice per condition. Therefore, a statistical *n* represents counts from multiple transplants of one differentiation experiment. Statistical significance was determined using a two-tailed Student's *t*-test.

A one-way ANOVA for SST:PV ratios of co-labeling with GFP over time at collection and mode of collection (mCherry or GFP) was calculated using StatPlusPro (AnalystSoft). The false discovery rate for both data sets was <0.0001. For each time point (DD12, 14 or 17) PV and SST fate ratios were calculated from at least three brains.

Slice preparation

Brain slices were prepared from mice (60-70 DPT) as described (Goldberg et al., 2011). Slices (275 µm thick) were cut on a microtome (Leica VT1200S) and incubated in a holding chamber at 32°C for 30 min, then at room temperature prior to recording. Artificial cerebrospinal fluid (ACSF) used for recording contained: 125 mM NaCl, 2.5 mM KCl, 1.25 mM NaH_2PO_4, 26 mM $NaHCO_3$, 10 mM glucose, 2 mM $CaCl_2$ and 1 mM $MgSO_4$.

Electrophysiological recordings

GFP-expressing neurons were visualized using a 40× water-immersion objective on an Olympus BX-51 upright microscope. Current clamp recordings were performed using the whole-cell patch-clamp technique. Access resistance (R_s) was <25 MΩ upon break-in; data obtained from a given cell were rejected if R_s changed by >20% during the experiment. Internal solution contained: 130 mM potassium gluconate; 6.3 mM potassium chloride; 0.5 mM EGTA; 1.0 mM $MgCl_2$; 10 mM HEPES; 4 mM Mg-ATP; 0.3 mM Na-GTP. Osmolarity was adjusted to 285-290 mOsm using 30% sucrose. Voltage was recorded using a MultiClamp 700B amplifier (Molecular Devices), low-pass-filtered at 10 kHz, digitized at 16-bit resolution (Digidata 1440) and sampled at 20 kHz. Data were acquired and analyzed using pCLAMP 10 software and Clampfit (Axon Instruments). RMP (V_m) was defined as the mean membrane potential during a 10-s baseline current clamp recording; membrane resistance (R_m) was calculated as the slope of the linear fit of the voltage/current relation near V_m; action potential half-width (AP 1/2-width) was calculated as the width of the AP at half maximal amplitude from AP threshold to peak of the AP; spike frequency adaptation was calculated as the ratio of the first to the tenth (ISI_1/ISI_{10}) or last (ISI_1/ISI_n) peak-to-peak interspike interval. For post-recording immunocytochemistry, 0.5% neurobiotin (Vector Labs) was included in the internal solution. Slices were fixed in 4% PFA for 4 h and subjected to immunofluorescence analysis for neurobiotin (streptavidin-conjugated 546, Jackson), and either PV (mouse anti-PV, Millipore; donkey anti-mouse Cy5) for FS cells (6 of 14 recorded) or somatostatin (rat anti-SST, Millipore; donkey anti-rat Cy5, Jackson) for the non-FS cells (8 of 14).

Acknowledgements

We thank the WCMC flow cytometry core, the CHOP stem cell core, the MSKCC molecular cytogenetics core, D. Alden, E. Ribeiro, D. Chinta, S. Milrad, F. Siddiqi, D. Tischfield, R. Mascereno, D. Feingold and J. Parker for technical assistance.

Competing interests

The authors declare no competing or financial interests.

Author contributions

J.A.T., E.M.G., A.M.M., T.J.P. and Q.X. conducted experiments and contributed to writing or editing the manuscript. J.A.T., E.M.G. and S.A.A. designed experiments. S.A.A. contributed to writing, editing and revising the manuscript.

Funding

This work was supported by the National Institutes of Health [R01 MH066912-01 to S.A.; NSADA K12NS049453 to E.M.G.; and T32 1T32HD060600 to J.T.]. Deposited in PMC for release after 12 months.

Supplementary material

Supplementary material available online at
http://dev.biologists.org/lookup/suppl/doi:10.1242/dev.111526/-/DC1

References

Au, E., Ahmed, T., Karayannis, T., Biswas, S., Gan, L. and Fishell, G. (2013). A modular gain-of-function approach to generate cortical interneuron subtypes from ES cells. *Neuron* **80**, 1145-1158.

Azim, E., Jabaudon, D., Fame, R. M. and Macklis, J. D. (2009). SOX6 controls dorsal progenitor identity and interneuron diversity during neocortical development. *Nat. Neurosci.* **12**, 1238-1247.

Batista-Brito, R. and Fishell, G. (2009). The developmental integration of cortical interneurons into a functional network. *Curr. Top. Dev. Biol.* **87**, 81-118.

Batista-Brito, R., Rossignol, E., Hjerling-Leffler, J., Denaxa, M., Wegner, M., Lefebvre, V., Pachnis, V. and Fishell, G. (2009). The cell-intrinsic requirement of Sox6 for cortical interneuron development. *Neuron* **63**, 466-481.

Belforte, J. E., Zsiros, V., Sklar, E. R., Jiang, Z., Yu, G., Li, Y., Quinlan, E. M. and Nakazawa, K. (2010). Postnatal NMDA receptor ablation in corticolimbic interneurons confers schizophrenia-like phenotypes. *Nat. Neurosci.* **13**, 76-83.

Binaschi, A., Bregola, G. and Simonato, M. (2003). On the role of somatostatin in seizure control: clues from the hippocampus. *Rev. Neurosci.* **14**, 285-301.

Butt, S. J. B., Fuccillo, M., Nery, S., Noctor, S., Kriegstein, A., Corbin, J. G. and Fishell, G. (2005). The temporal and spatial origins of cortical interneurons predict their physiological subtype. *Neuron* **48**, 591-604.

Butt, S. J. B., Sousa, V. H., Fuccillo, M. V., Hjerling-Leffler, J., Miyoshi, G., Kimura, S. and Fishell, G. (2008). The requirement of Nkx2-1 in the temporal specification of cortical interneuron subtypes. *Neuron* **59**, 722-732.

Cavanagh, M. E. and Parnavelas, J. G. (1988). Development of somatostatin immunoreactive neurons in the rat occipital cortex: a combined immuno-cytochemical-autoradiographic study. *J. Comp. Neurol.* **268**, 1-12.

Chao, H.-T., Chen, H., Samaco, R. C., Xue, M., Chahrour, M., Yoo, J., Neul, J. L., Gong, S., Lu, H.-C., Heintz, N. et al. (2010). Dysfunction in GABA signalling mediates autism-like stereotypies and Rett syndrome phenotypes. *Nature* **468**, 263-269.

Chen, Y.-J., Vogt, D., Wang, Y., Visel, A., Silberberg, S. N., Nicholas, C. R., Danjo, T., Pollack, J. L., Pennacchio, L. A., Anderson, S. et al. (2013). Use of "MGE Enhancers" for labeling and selection of embryonic stem cell-derived Medial Ganglionic Eminence (MGE) progenitors and neurons. *PLoS ONE* **8**, e61956.

Danjo, T., Eiraku, M., Muguruma, K., Watanabe, K., Kawada, M., Yanagawa, Y., Rubenstein, J. L. R. and Sasai, Y. (2011). Subregional specification of embryonic stem cell-derived ventral telencephalic tissues by timed and combinatory treatment with extrinsic signals. *J. Neurosci.* **31**, 1919-1933.

DeFelipe, J., López-Cruz, P. L., Benavides-Piccione, R., Bielza, C., Larrañaga, P., Anderson, S., Burkhalter, A., Cauli, B., Fairén, A., Feldmeyer, D. et al. (2013). New insights into the classification and nomenclature of cortical GABAergic interneurons. *Nat. Rev. Neurosci.* **14**, 202-216.

Du, T., Xu, Q., Ocbina, P. J. and Anderson, S. A. (2008). NKX2.1 specifies cortical interneuron fate by activating Lhx6. *Development* **135**, 1559-1567.
Fancy, S. P. J., Harrington, E. P., Yuen, T. J., Silbereis, J. C., Zhao, C., Baranzini, S. E., Bruce, C. C., Otero, J. J., Huang, E. J., Nusse, R. et al. (2011). Axin2 as regulatory and therapeutic target in newborn brain injury and remyelination. *Nat. Neurosci.* **14**, 1009-1016.
Fino, E., Packer, A. M. and Yuste, R. (2013). The logic of inhibitory connectivity in the neocortex. *Neuroscientist* **19**, 228-237.
Flames, N., Pla, R., Gelman, D. M., Rubenstein, J. L. R., Puelles, L. and Marin, O. (2007). Delineation of multiple subpallial progenitor domains by the combinatorial expression of transcriptional codes. *J. Neurosci.* **27**, 9682-9695.
Flandin, P., Kimura, S. and Rubenstein, J. L. R. (2010). The progenitor zone of the ventral medial ganglionic eminence requires Nkx2-1 to generate most of the globus pallidus but few neocortical interneurons. *J. Neurosci.* **30**, 2812-2823.
Flandin, P., Zhao, Y., Vogt, D., Jeong, J., Long, J., Potter, G., Westphal, H. and Rubenstein, J. L. R. (2011). Lhx6 and Lhx8 coordinately induce neuronal expression of Shh that controls the generation of interneuron progenitors. *Neuron* **70**, 939-950.
Fogarty, M., Grist, M., Gelman, D., Marin, O., Pachnis, V. and Kessaris, N. (2007). Spatial genetic patterning of the embryonic neuroepithelium generates GABAergic interneuron diversity in the adult cortex. *J. Neurosci.* **27**, 10935-10946.
Fuccillo, M., Rallu, M., McMahon, A. P. and Fishell, G. (2004). Temporal requirement for hedgehog signaling in ventral telencephalic patterning. *Development* **131**, 5031-5040.
Gaspard, N. and Vanderhaeghen, P. (2011). From stem cells to neural networks: recent advances and perspectives for neurodevelopmental disorders. *Dev. Med. Child Neurol.* **53**, 13-17.
Gelman, D. M., Martini, F. J., Nobrega-Pereira, S., Pierani, A., Kessaris, N. and Marin, O. (2009). The embryonic preoptic area is a novel source of cortical GABAergic interneurons. *J. Neurosci.* **29**, 9380-9389.
Glickstein, S. B., Moore, H., Slowinska, B., Racchumi, J., Suh, M., Chuhma, N. and Ross, M. E. (2007). Selective cortical interneuron and GABA deficits in cyclin D2-null mice. *Development* **134**, 4083-4093.
Glinka, A., Wu, W., Delius, H., Monaghan, A. P., Blumenstock, C. and Niehrs, C. (1998). Dickkopf-1 is a member of a new family of secreted proteins and functions in head induction. *Nature* **391**, 357-362.
Goldberg, E. M., Jeong, H. Y., Kruglikov, I., Tremblay, R., Lazarenko, R. M. and Rudy, B. (2011). Rapid developmental maturation of neocortical FS cell intrinsic excitability. *Cereb. Cortex* **21**, 666-682.
Goulburn, A. L., Alden, D., Davis, R. P., Micallef, S. J., Ng, E. S., Yu, Q. C., Lim, S. M., Soh, C. L., Elliott, D. A., Hatzistavrou, T. et al. (2011). A targeted NKX2.1 Hesc reporter line enables identification of human basal forebrain derivatives. *Stem Cells* **29**, 462-473.
Goulburn, A. L., Stanley, E. G., Elefanty, A. G. and Anderson, S. A. (2012). Generating GABAergic cerebral cortical interneurons from mouse and human embryonic stem cells. *Stem Cell Res.* **8**, 416-426.
Hébert, J. M. and Fishell, G. (2008). The genetics of early telencephalon patterning: some assembly required. *Nat. Rev. Neurosci.* **9**, 678-685.
Houart, C., Caneparo, L., Heisenberg, C.-P., Barth, K. A., Take-Uchi, M. and Wilson, S. W. (2002). Establishment of the telencephalon during gastrulation by local antagonism of Wnt signaling. *Neuron* **35**, 255-265.
Huang, S.-M. A., Mishina, Y. M., Liu, S., Cheung, A., Stegmeier, F., Michaud, G. A., Charlat, O., Wiellette, E., Zhang, Y., Wiessner, S. et al. (2009). Tankyrase inhibition stabilizes axin and antagonizes Wnt signalling. *Nature* **461**, 614-620.
Inan, M., Welagen, J. and Anderson, S. A. (2012). Spatial and temporal bias in the mitotic origins of somatostatin- and parvalbumin-expressing interneuron subgroups and the chandelier subtype in the medial ganglionic eminence. *Cereb. Cortex* **22**, 820-827.
Inan, M., Petros, T. J. and Anderson, S. A. (2013). Losing your inhibition: linking cortical GABAergic interneurons to schizophrenia. *Neurobiol. Dis.* **53**, 36-48.
Jiang, Z., Cowell, R. M. and Nakazawa, K. (2013). Convergence of genetic and environmental factors on parvalbumin-positive interneurons in schizophrenia. *Front. Behav. Neurosci.* **7**, 116.
Kawaguchi, Y. and Kubota, Y. (1996). Physiological and morphological identification of somatostatin- or vasoactive intestinal polypeptide-containing cells among GABAergic cell subtypes in rat frontal cortex. *J. Neurosci.* **16**, 2701-2715.
Kawaguchi, Y. and Kubota, Y. (1997). GABAergic cell subtypes and their synaptic connections in rat frontal cortex. *Cereb. Cortex* **7**, 476-486.
Lamba, D. A., Karl, M. O., Ware, C. B. and Reh, T. A. (2006). Efficient generation of retinal progenitor cells from human embryonic stem cells. *Proc. Natl. Acad. Sci. USA* **103**, 12769-12774.
Lavdas, A. A., Grigoriou, M., Pachnis, V. and Parnavelas, J. G. (1999). The medial ganglionic eminence gives rise to a population of early neurons in the developing cerebral cortex. *J. Neurosci.* **19**, 7881-7888.
Lee, S., Hjerling-Leffler, J., Zagha, E., Fishell, G. and Rudy, B. (2010). The largest group of superficial neocortical GABAergic interneurons expresses ionotropic serotonin receptors. *J. Neurosci.* **30**, 16796-16808.
Lehmann, K., Steinecke, A. and Bolz, J. (2012). GABA through the ages: regulation of cortical function and plasticity by inhibitory interneurons. *Neural Plast.* **2012**, 892784.
Levitt, P., Eagleson, K. L. and Powell, E. M. (2004). Regulation of neocortical interneuron development and the implications for neurodevelopmental disorders. *Trends Neurosci.* **27**, 400-406.
Liodis, P., Denaxa, M., Grigoriou, M., Akufo-Addo, C., Yanagawa, Y. and Pachnis, V. (2007). Lhx6 activity is required for the normal migration and specification of cortical interneuron subtypes. *J. Neurosci.* **27**, 3078-3089.
Lodato, S., Tomassy, G. S., De Leonibus, E., Uzcategui, Y. G., Andolfi, G., Armentano, M., Touzot, A., Gaztelu, J. M., Arlotta, P., Menendez de la Prida, L. et al. (2011). Loss of COUP-TFI alters the balance between caudal ganglionic eminence- and medial ganglionic eminence-derived cortical interneurons and results in resistance to epilepsy. *J. Neurosci.* **31**, 4650-4662.
Maisano, X., Litvina, E., Tagliatela, S., Aaron, G. B., Grabel, L. B. and Naegele, J. R. (2012). Differentiation and functional incorporation of embryonic stem cell-derived GABAergic interneurons in the dentate gyrus of mice with temporal lobe epilepsy. *J. Neurosci.* **32**, 46-61.
Mao, B., Wu, W., Li, Y., Hoppe, D., Stannek, P., Glinka, A. and Niehrs, C. (2001). LDL-receptor-related protein 6 is a receptor for Dickkopf proteins. *Nature* **411**, 321-325.
Marin, O., Anderson, S. A. and Rubenstein, J. L. (2000). Origin and molecular specification of striatal interneurons. *J. Neurosci.* **20**, 6063-6076.
Maroof, A. M., Brown, K., Shi, S. H., Studer, L. and Anderson, S. A. (2010). Prospective isolation of cortical interneuron precursors from mouse embryonic stem cells. *J. Neurosci.* **30**, 4667-4675.
Maroof, A. M., Keros, S., Tyson, J. A., Ying, S.-W., Ganat, Y. M., Merkle, F. T., Liu, B., Goulburn, A., Stanley, E. G., Elefanty, A. G. et al. (2013). Directed differentiation and functional maturation of cortical interneurons from human embryonic stem cells. *Cell Stem Cell* **12**, 559-572.
Nicholas, C. R., Chen, J., Tang, Y., Southwell, D. G., Chalmers, N., Vogt, D., Arnold, C. M., Chen, Y.-J. J., Stanley, E. G., Elefanty, A. G. et al. (2013). Functional maturation of hPSC-derived forebrain interneurons requires an extended timeline and mimics human neural development. *Cell Stem Cell* **12**, 573-586.
Niehrs, C. (2006). Function and biological roles of the Dickkopf family of Wnt modulators. *Oncogene* **25**, 7469-7481.
Nóbrega-Pereira, S., Kessaris, N., Du, T., Kimura, S., Anderson, S. A. and Marín, O. (2008). Postmitotic Nkx2-1 controls the migration of telencephalic interneurons by direct repression of guidance receptors. *Neuron* **59**, 733-745.
Ohkubo, Y., Chiang, C. and Rubenstein, J. L. R. (2002). Coordinate regulation and synergistic actions of BMP4, SHH and FGF8 in the rostral prosencephalon regulate morphogenesis of the telencephalic and optic vesicles. *Neuroscience* **111**, 1-17.
Petros, T. J., Maurer, C. W. and Anderson, S. A. (2013). Enhanced derivation of mouse ESC-derived cortical interneurons by expression of Nkx2.1. *Stem Cell Res.* **11**, 647-656.
Rudy, B., Fishell, G., Lee, S. and Hjerling-Leffler, J. (2011). Three groups of interneurons account for nearly 100% of neocortical GABAergic neurons. *Dev. Neurobiol.* **71**, 45-61.
Rymar, V. V. and Sadikot, A. F. (2007). Laminar fate of cortical GABAergic interneurons is dependent on both birthdate and phenotype. *J. Comp. Neurol.* **501**, 369-380.
Shimogori, T., Banuchi, V., Ng, H. Y., Strauss, J. B. and Grove, E. A. (2004). Embryonic signaling centers expressing BMP, WNT and FGF proteins interact to pattern the cerebral cortex. *Development* **131**, 5639-5647.
Smith-Hicks, C. L. (2013). GABAergic dysfunction in pediatric neuro-developmental disorders. *Front. Cell. Neurosci.* **7**, 269.
Sousa, V. H., Miyoshi, G., Hjerling-Leffler, J., Karayannis, T. and Fishell, G. (2009). Characterization of Nkx6-2-derived neocortical interneuron lineages. *Cereb. Cortex* **19** Suppl. 1, i1-i10.
Southwell, D. G., Nicholas, C. R., Basbaum, A. I., Stryker, M. P., Kriegstein, A. R., Rubenstein, J. L. and Alvarez-Buylla, A. (2014). Interneurons from embryonic development to cell-based therapy. *Science* **344**, 1240622.
Sussel, L., Marin, O., Kimura, S. and Rubenstein, J. L. (1999). Loss of Nkx2.1 homeobox gene function results in a ventral to dorsal molecular respecification within the basal telencephalon: evidence for a transformation of the pallidum into the striatum. *Development* **126**, 3359-3370.
Tamamaki, N., Yanagawa, Y., Tomioka, R., Miyazaki, J.-I., Obata, K. and Kaneko, T. (2003). Green fluorescent protein expression and colocalization with calretinin, parvalbumin, and somatostatin in the GAD67-GFP knock-in mouse. *J. Comp. Neurol.* **467**, 60-79.
Tomishima, M. J., Hadjantonakis, A.-K., Gong, S. and Studer, L. (2007). Production of green fluorescent protein transgenic embryonic stem cells using the GENSAT bacterial artificial chromosome library. *Stem Cells* **25**, 39-45.
Tyson, J. A. and Anderson, S. A. (2014). GABAergic interneuron transplants to study development and treat disease. *Trends Neurosci.* **37**, 169-177.
Vogt, D., Hunt, R. F., Mandal, S., Sandberg, M., Silberberg, S. N., Nagasawa, T., Yang, Z., Baraban, S. C. and Rubenstein, J. L. R. (2014). Lhx6 directly regulates

Development (2015) 142, 1267-1278 doi:10.1242/dev.111526

Arx and CXCR7 to determine cortical interneuron fate and laminar position. *Neuron* **82**, 350-364.

Watanabe, K., Kamiya, D., Nishiyama, A., Katayama, T., Nozaki, S., Kawasaki, H., Watanabe, Y., Mizuseki, K. and Sasai, Y. (2005). Directed differentiation of telencephalic precursors from embryonic stem cells. *Nat. Neurosci.* **8**, 288-296.

Wonders, C. P., Taylor, L., Welagen, J., Mbata, I. C., Xiang, J. Z. and Anderson, S. A. (2008). A spatial bias for the origins of interneuron subgroups within the medial ganglionic eminence. *Dev. Biol.* **314**, 127-136.

Xu, Q., Cobos, I., De La Cruz, E., Rubenstein, J. L. and Anderson, S. A. (2004). Origins of cortical interneuron subtypes. *J. Neurosci.* **24**, 2612-2622.

Xu, Q., Wonders, C. P. and Anderson, S. A. (2005). Sonic hedgehog maintains the identity of cortical interneuron progenitors in the ventral telencephalon. *Development* **132**, 4987-4998.

Xu, Q., Tam, M. and Anderson, S. A. (2008). Fate mapping Nkx2.1-lineage cells in the mouse telencephalon. *J. Comp. Neurol.* **506**, 16-29.

Xu, Q., Guo, L., Moore, H., Waclaw, R. R., Campbell, K. and Anderson, S. A. (2010a). Sonic hedgehog signaling confers ventral telencephalic progenitors with distinct cortical interneuron fates. *Neuron* **65**, 328-340.

Xu, X., Roby, K. D. and Callaway, E. M. (2010b). Immunochemical characterization of inhibitory mouse cortical neurons: three chemically distinct classes of inhibitory cells. *J. Comp. Neurol.* **518**, 389-404.

Zhao, Y., Flandin, P., Long, J. E., Cuesta, M. D., Westphal, H. and Rubenstein, J. L. R. (2008). Distinct molecular pathways for development of telencephalic interneuron subtypes revealed through analysis of Lhx6 mutants. *J. Comp. Neurol.* **510**, 79-99.